New On-Bead Near-Infrared Fluorophores and Fluorescent Sensor Constructs
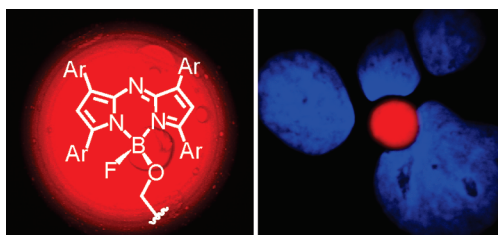
Aniello Palma,[†] Mariusz Tasior,[†] Daniel O. Frimannsson,[†] Thanh Truc Vu,[‡] Rachel Méallet-Renault,[‡] and Donal F. O'Shea*[,†]

Centre for Synthesis and Chemical Biology, School of Chemistry and Chemical Biology, University College Dublin, Belfield, Dublin 4, Ireland, and PPSM, ENS Cachan, CNRS, UniverSud, 61 av President Wilson, F-94230 Cachan, France

donal.f.oshea@ucd.ie

ABSTRACT

The facile synthesis and photophysical characterization of new on-bead fluorophores and fluorescent sensors are described. The unique covalent immobilization strategy results in highly fluorescent beads with sharp emission profiles between 650 and 800 nm. Illustrative examples include imaging in an aqueous cellular environment and adaptation to include off/on sensing functionality, proven by a prototypical detection of gaseous HCl.

The exploitation of organic fluorophores as reporters of dynamic biological and environmental processes is a vibrant research field.[1] The number of reported molecular fluorescent sensors that respond to key biological and environmental substrates is vast. Yet, despite the advantages offered, comparatively few have been immobilized (via covalent or noncovalent methods) on inert substrates (particles or beads).[2] Significant photophysical and application benefits can be accrued from immobilization, including improved brightness and photostability coupled with positional control of the label or sensor. Potential future *in vivo* biological applications can be envisaged for such constructs in which immobilized sensor implants provide a continuous real-time analyte read-out. Recently, the advent of particle-based labels and sensors has focused on noncovalently linked dye-doped polymers, which can suffer from fluorophore aggregation, self-quenching, and leaching. The development of covalently bound fluorophores is far more limited despite the potential to solve these limiting factors.[3] Our fluorophore class of choice is the BF_2 chelated tetraarylazadipyrromethene **1**, which has recently emerged as a new class of fluorophore that emits between 650 and 780 nm (Scheme 1).[4] These far visible red and near-infrared (NIR) spectral characteristics offer distinct advantages for both *in vitro* and *in vivo* biological use as they avoid the strong interference from endogenous chromophores encountered at lower wavelengths.[5] We and others have shown that with selective positioning of analyte receptors on the aryl

[†] University College Dublin.

[‡] PPSM, ENS Cachan.

(1) Rao, J.; Dragulescu-Andrasi, A; Yao, H. *Curr. Opin. Biotechnol.* **2007**, *18*, 17.

(2) (a) Copeland, G. T.; Miller, S. J. *J. Am. Chem. Soc.* **1999**, *121*, 4306. (b) Méallet-Renault, R.; Denjean, P.; Pansu, R. B. *Sens Actuators B* **1999**, *59*, 108. (c) Méallet-Renault, R.; Pansu, R.; Amigoni-Gerbier, S.; Larpent, C. *Chem. Commun.* **2004**, *20*, 2344. (d) Ow, H.; Larson, D. R.; Srivastava, M.; Baird, B. A.; Webb, W. W.; Wiesner, U. *Nano Lett.* **2005**, *5*, 113. (e) Nath, S.; Maitra, U. *Org. Lett.* **2006**, *8*, 3239. (f) Brown, G. J.; de Silva, A. P.; James, M. R.; McKinney, B. O. F.; Pears, D. A.; Weir, S. M. *Tetrahedron* **2008**, *64*, 8301.

(3) Tian, Z.; Shaller, A. D.; Li, A. D. Q. *Chem. Commun.* **2009**, *2*, 180.

(4) (a) Killoran, J.; Allen, L.; Gallagher, J. F.; Gallagher, W. M.; O'Shea,

rings of **1** this class can be utilized as a fluorosensor, operating by either a photoinduced electron transfer (PET) or an internal charge transfer (ICT) mechanism.[6]

A significant drawback to covalent immobilization of existing molecular fluorophores and sensors is the additional synthetic steps required to make the fluorophore−particle covalent bond. Typical approaches have utilized amide[2a,f] or ester[2e] bond formation on polymer beads or silicon−oxygen[2d] linkages on silica particles. It would be distinctly attractive if a fluorophore linking method existed that did not require any additional synthetic complexity. Herein we report our first set of data acquired in pursuit of this goal for the fluorophore class **1** with biologically inert polystyrene beads of various sizes (5−150 μm). Our unique linking strategy was to employ the reaction of alcohol-functionalized polystyrene beads with **1** to effect an oxygen for fluorine displacement, thereby generating a fluorophore−boron−oxygen−polymer bead linked construct **2** (Scheme 1). Intramolecular oxygen−fluorine displacement reactions on this compound class have recently been reported.[7]

Scheme 1. Strategy for Covalent Linkage
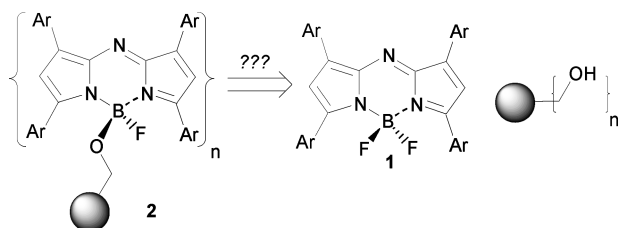
Mild reaction conditions were first optimized for the intermolecular fluorine displacement reaction of **1a−c** with methanol with the goal of utilizing these conditions for bead functionalization.[8] It was found that the treatment of a THF solution of **1a−c** with 3 equiv of NaH and 10 equiv of MeOH at rt for 16 h was an efficient method for substitution of both fluorine atoms to provide **3a−c**, as bench-stable solids, following chromatographic purification (Scheme 2, Supporting Information).

D. F. *Chem. Commun.* **2002**, *17*, 1862. (b) Gorman, A.; Killoran, J.; O'Shea, C.; Kenna, T.; Gallagher, W. M.; O'Shea, D. F. *J. Am. Chem. Soc.* **2004**, *126*, 10619. (c) McDonnell, S. O.; Hall, M. J.; Allen, L. T.; Byrne, A.; Gallagher, W. M.; O'Shea, D. F. *J. Am. Chem. Soc.* **2005**, *127*, 16360. (d) Gallagher, W. M.; Allen, L. T.; O'Shea, C.; Kenna, T.; Hall, M.; Killoran, J.; O'Shea, D. F. *Br. J. Cancer* **2005**, *92*, 1702. (e) Hall, M. J.; McDonnell, S. O.; Killoran, J.; O'Shea, D. F. *J. Org. Chem.* **2005**, *70*, 5571.
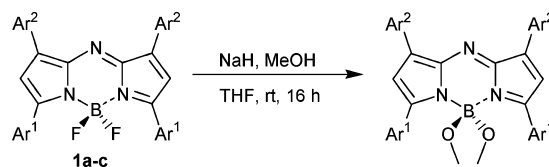 (5) Ntziachristos, V.; Ripoll, J.; Wang, L. V.; Weissleder, R. *Nat. Biotechnol.* **2005**, *23*, 313.
  (6) (a) Killoran, J.; O'Shea, D. F. *Chem. Commun.* **2006**, *14*, 1503. (b) Hall, M. J.; Allen, L. T.; O'Shea, D. F. *Org. Biomol. Chem.* **2006**, *4*, 776. (c) McDonnell, S. O.; O'Shea, D. F. *Org. Lett.* **2006**, *8*, 3493. (d) Gawley, R. E.; Mao, H.; Mahbubul Haque, M.; Thorne, J. B.; Pharr, J. S. *J. Org. Chem.* **2007**, *72*, 2187. (e) Coskun, A.; Deniz Yilmaz, M.; Akkaya, E. U. *Org. Lett.* **2007**, *9*, 607. (f) Loudet, A.; Bandichhor, R.; Wu, L.; Burgess, K. *Tetrahedron* **2008**, *64*, 3642. (g) Killoran, J.; McDonnell, S. O.; Gallagher, J. F.; O'Shea, D. F. *New J. Chem.* **2008**, *32*, 483.
  (7) Loudet, A.; Bandichhor, R.; Burgess, K.; Palma, A.; McDonnell, S. O.; Hall, M. J.; O'Shea, D. F. *Org. Lett.* **2008**, *21*, 4772.
  (8) For conditions utilized in oxygen-fluorine displacements on BODIPY dyes, see: (a) Gabe, Y.; Ueno, T.; Kojima, H.; Nagano, T. *Anal. Bioanal. Chem.* **2006**, *386*, 621. (b) Tahtaoui, C.; Thomas, C.; Rohmer, F.; Klotz, P.; Duportail, G.; Mly, Y.; Bonnet, D.; Hibert, M. *J. Org. Chem.* **2007**, *72*, 269.

Scheme 2. Synthesis of B(OMe)$_2$ Derivatives

entry	1	Ar^1	Ar^2	3	yield (%)
1	a	C$_6$H$_5$	C$_6$H$_5$	a	65
2	b	p-CH$_3$OC$_6$H$_4$	C$_6$H$_5$	b	60
3	c	C$_6$H$_5$	p-(CH$_3$)$_2$NC$_6$H$_4$	c	30

We were pleased to observe that the spectral properties of **3a−c** did not significantly change from their corresponding BF$_2$ chelated derivatives **1a−c** (Table 1, Supporting Information).[4b,6g] Specifically, the λ_{max} emissions for **3a** and **3b** were recorded at 674 and 711 nm, respectively, with fluorescence quantum yields (ϕ) of 0.31 and 0.30 (Table 1; entries 5 and 6). This shows little difference from the corresponding BF$_2$ analogues **1a** and **2a** (entries 1 and 2, Supporting Information).[4b] We have previously reported that the bis-anilino substituted **1c** can act as a fluorosensor with fluorescence signal modulated in response to acidic protonation of both anilines (Table 1; entries 3 and 4).[6g] Similar behavior was observed for **3c** for which the fluorescence output between 660 and 760 nm was virtually completely quenched as a consequence of the donor−acceptor charge transfer between the anilino lone pairs of electrons and the fluorophore (Table 1; entries 7 and 8, Supporting Information). Upon protonation to **3c**-2H$^+$, with TFA, the fluorescence spectrum showed a strong proton-induced fluorescence enhancement with a wavelength of maximum fluorescence at 684 nm (entry 8, Supporting Information). Significantly, the fluorescence enhancement factor (FEF) was greater than 250-fold.

**Table 1.** Comparative Spectral Characteristics of **1a−c** and **3a−c**^{a}

entry	compd	abs λ_{max} (nm)	fluor λ_{max} (nm)	ϕ_f
1	**1a**^{4b}	650	672	0.34
2	**1b**^{4b}	688	715	0.36
3	**1c**^{6g}	770, 625	820^b	
4	**1c**-2H^{+6g}	650	684^d	
5	**3a**	649	674	0.31^c
6	**3b**	674	711	0.30^c
7	**3c**	733, 620	822^b	
8	**3c**-2H$^+$	644	684^d	

^{a} In CHCl$_3$. ^{b} Very weak CT emission (Supporting Information). ^{c} **1a,b** used as references. ^{d} In CHCl$_3$ with TFA.

To transfer these spectral features to polymeric beads, 1% cross-linked polystyrene beads of 150 μm size (Wang resin beads with 0.9 mmol/g loading) and smaller 5 μm variants were used as illustrative examples. The developed protocol treated a THF suspension of the beads with 1 equiv of NaH for 20 min at rt followed by 0.5 equiv of **1a−c** (Scheme 3).

The suspension was agitated for 16 h at rt, and the beads were filtered and washed successively three times with dichloromethane and THF (Supporting Information).

Scheme 3. Polystyrene Bead Functionalization
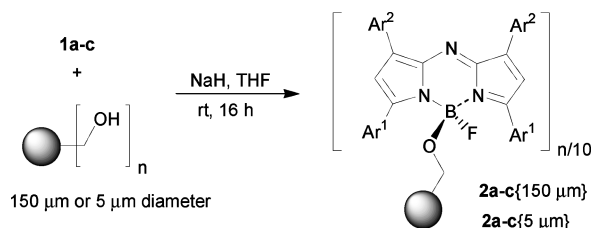
The dried beads of **2a−c**{150 μm} and **2a−c**{5 μm} had a blue-black color and were stored at rt without any precautions. An estimated 10% of reactive alcohol sites were functionalized on the basis of recovered starting material.[9] It was anticipated that this level of dye loading would be sufficient as higher loading levels may result in self-quenching.
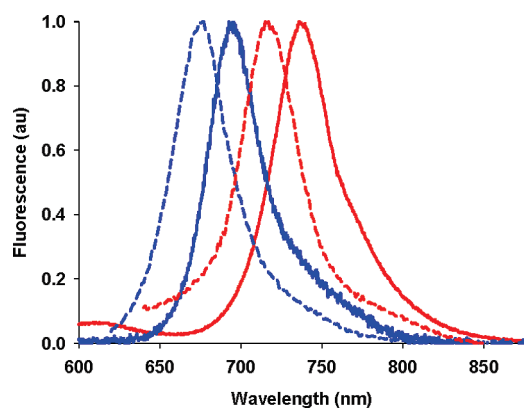

Figure 1. Normalized fluorescence spectra (excitation at 515 nm with a focused laser beam) from a single dry bead of **2a**{150 μm} (solid blue trace) and **2b**{150 μm} (solid red trace). Normalized fluorescence spectra (excitation at 630 nm) taken as a suspension in toluene of **2a**{5 μm} (dashed blue trace) and **2b**{5 μm} (dashed red trace).

Spectroscopic analysis of numerous individual dry beads of **2a**{150 μm} and **2b**{150 μm} gave uniform bead to bead emission spectra with λ maxima at 696 and 736 nm, respectively, following laser excitation at 515 nm (Figure 1, Table 2 entries 1 and 2). These emission profiles are similar to those of the constituent fluorophores **3a,b** in solution but have a favorable bathochromic shift of 22 and 25 nm, respectively. Emission spectra of **2a,b**{5 μm}, taken as a suspension in toluene, gave similar profiles with a less

(9) The principal mode of linking is expected via one boron−oxygen bond linkage though double linked fluorophore, i.e., B-(O)$_2$-bead is also possible.

Table 2. On-Bead Emission Parameters

entry	compd	bead size (μm)	fluor λ_{max} (nm)
1	**2a**	150	696[a]
2	**2b**	150	736[a]
3	**2c**	150	[a]
4	**2c**-2H$^+$	150	701[b]
5	**2a**	5	680[c]
6	**2b**	5	718[c]
7	**2c**	5	[c]
8	**2c**-2H$^+$	5	694[d]

[a] Spectra taken from dry bead. [b] Spectra taken from dry bead treated with HCl$_{(g)}$. [c] Spectra taken in toluene. [d] Spectra taken in toluene with TFA.

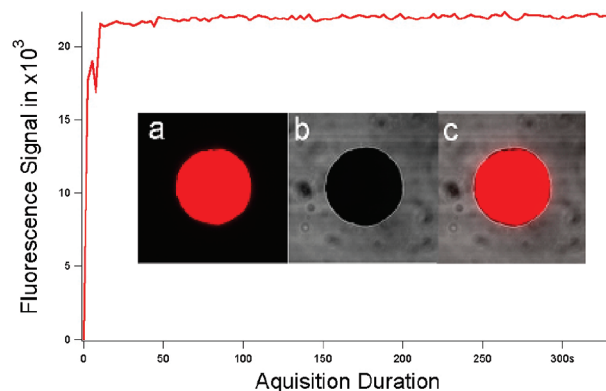pronounced bathochromic shift when compared to **3a,b** (entries 5 and 6).

Figure 2. Inset: (a) CLSM image using 633 nm excitation and 650 nm long-pass collection filter, (b) transmittance image, (c) overlay of (a) and (b) of a single dry bead of **2a**{150 μm}. Graphed plot: Photobleaching experiment for **2a**{150 μm} showing fluorescence output during continuous irradiation at 515 nm with 3.3 mW of laser power for 10 min.

Three-dimensional single bead visualizations of **2a,b**{150 μm} were carried out using confocal laser scanning microscopy (CLSM). Both proved to be highly fluorescent when excited by a 633 nm helium neon laser and emission collected using a 650 nm long pass filter (Figure 2, Supporting Information). The emission profile throughout a single bead of **2a** was obtained by optical cross-sectional analysis of 98 individual focal planes 0.56 μm apart (Supporting Information). This analysis showed emission throughout the bead, however, with significantly lower emission from the center of the bead due to an expected self-quenching.[10] Both **2a,b**{150 μm} had exceptional photostability with no loss in fluorescence signal during continuous irradiation with intensive laser power for prolonged time periods (Figure 2, graphed plot, Supporting Information).

The ability to clearly detect the 5 μm beads in aqueous cellular environments has been achieved. Following the

(10) Rademann, J.; Barth, M.; Brock, R.; Egelhaaf, H.-J.; Jung, G *Chem.—Eur. J.* **2001**, 7, 3884.

incubation of **2a**{5 μm} beads with MDA cells for 8 h, the nuclei of the cells were stained blue with 4,6-diamidino-2-phenylindole (DAPI) and fluorescent images were captured by CLSM (Figure 3).

Multiple red fluorescent beads were clearly visible in an extracellular environment as would be anticipated for particles of this size (Figure 3, top panel). The lower panel of Figure 3 shows a higher resolution image of a single bead surrounded by cells with a blue DAPI nuclear stain.
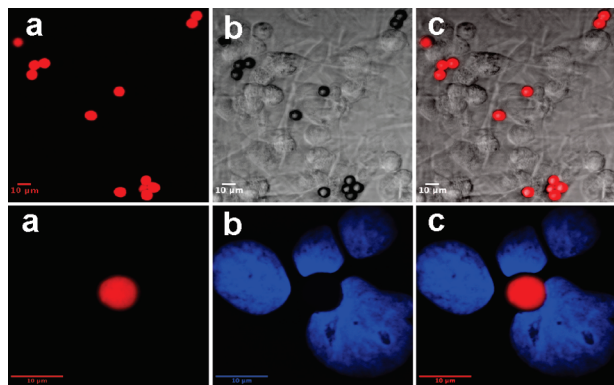

Figure 3. CLSM images of **2a**{5 μm} beads with MDA cells costained with DAPI. Top panel: (a) CLSM image, (b) transmittance image, (c) overlay of (a) and (b). Bottom panel: CLSM image of (a) a single bead with 633 nm excitation and a 650 nm long-pass collection filter and (b) with 365 nm excitation and 385−470 nm band-pass filter showing blue DAPI nuclear stain, (c) overlay of (a) and (b).

The inclusion of amine substituents on fluorophore **3c** provided an acid-responsive fluorosensor for which a large FEF was recorded in solution (Table 1, entries 7 and 8, Supporting Information). It would be of considerable advantage if these characteristics could be integrated onto a bead that resulted in pronounced emission changes by the entire bead due to a substrate recognition event. Examination of the emission properties of **2c**{5 μm} beads as suspensions in solution and **2c**{150 μm} as single dry beads showed that this is the case. Spectroscopic analysis of toluene suspensions of **2c**{5 μm} revealed almost complete quenching of the fluorescence signal (Figure 4, green trace; Table 2, entry 7). Upon protonation by sequential addition of aliquots of TFA the fluorescence spectrum showed a strong proton-induced fluorescence enhancement with wavelength of maximum fluorescence at 694 nm and an FEF greater than 100 (Figure 4, red trace; Table 2, entry 8).

CLSM bead analysis of **2c**{150 μm} showed a very weak emission illustrating that ICT quenching was effective at suppressing emission from the entire bead (Figure 5, top; a, b, c). Validation of the prototypical on-bead sensing ability was achieved by determining the response to an acid analyte. Dry beads of **2c**{150 μm} were placed in a sample vial and exposed to HCl gas for 5 min and re-examined by CLSM. The analyte-induced response was readily observable with fluorescence of the entire bead clearly re-established with a calculated FEF of greater than 50 (Figure 5, bottom; d, e, f, Supporting Information). The emission spectrum of beads exposed to HCl gave the expected band with a λ_{max} of 701 nm (Figure 4, inset).
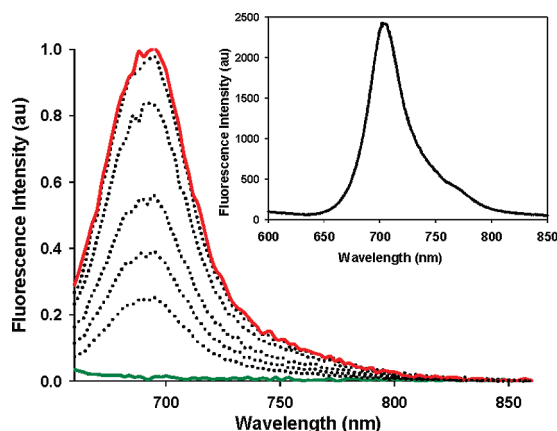
Figure 4. Normalized fluorescence spectra (excitation at 630 nm) of a toluene suspension of **2c**{5 μm} beads with successive additions of TFA. Inset: fluorescence spectrum (excitation at 515 nm with a focused laser beam) from a single dry bead of **2c**{150 μm} following treatment with $HCl_{(g)}$.

In conclusion, a new covalent linking of NIR fluorophores and sensors to polymeric beads has been successfully demonstrated. The beads exhibit excellent photophysical properties and have the ability to act as off/on sensors. Extension of these concepts to other particle types and analyte/receptor combinations for specific uses is ongoing.
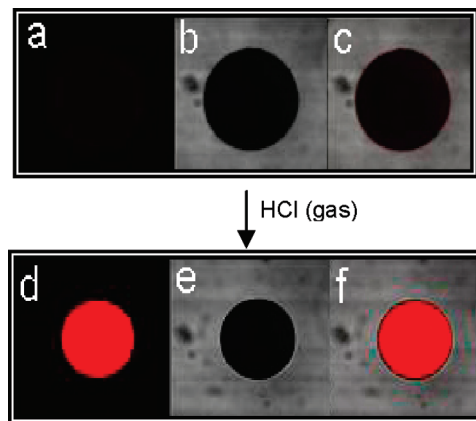

Figure 5. On bead sensor. Top: (a) CLSM image using 633 nm laser excitation and 650 nm long-pass collection filter of a single dry bead of **2c**{150 μm}, (b) transmittance image, (c) overlay of (a) and (b). Bottom: (d) CLSM image of a single dry bead of **2c**{150 μm} following treatment with $HCl_{(g)}$, (e) transmittance image, (f) overlay of (d) and (e).

Supporting Information Available: Experimental and analytical data. This material is available free of charge via the Internet at http://pubs.acs.org.

OL901413U